Welding in the World (2021) 65:381–392
https://doi.org/10.1007/s40194-020-01035-6

RESEARCH PAPER

Hot cracking tendency of flux-cored arc welding with flux-cored wires of types Ni 6625

Stefan Burger[1] · Manuela Zinke[1] · Sven Jüttner[1]

Received: 31 July 2020 / Accepted: 21 November 2020 / Published online: 15 January 2021

Abstract
Due to their mechanical and corrosive properties, nickel-based alloys are very important in several industrial sectors like power stations, chemical apparatus, and the oil industry. While flux-cored arc welding (FCAW) of carbon steels often uses flux-cored wires (FCW), the use of Ni-based flux-cored wires is industrially less common. The reasons for this include the lower degree of recognition and the higher material costs compared to solid wires. In comparison to solid wires, flux-cored wires have some technological benefits such as the possibility of welding without pulsed arc technology using low-cost standard mixed gases, which has a much lower tendency to weld defects due to high penetration depth. Depending on the slag, the flux-cored wires have a good weldability and excellent mechanical properties. Based on the self-stressed and externally stressed hot crack tests, the basic FCW showed a higher hot cracking susceptibility, contrary to the original assumption. Even if the causes have not yet been finally clarified, a negative influence of the comparatively high sulfur and oxygen contents in the basic FCW is suspected. The weld metal of the solid wires showed the highest hot crack resistance.

Keywords Hot crack · Nickel alloys · Flux-cored wires · Weldability tests

1 Introduction

Welding of nickel-based alloys is often problematic because of their sensitivity to the occurrence of hot cracks and lack of fusion in the welds [1, 2]. The hot cracking behavior is known to be influenced by three factors metallurgy, welding method, and structural mechanics [3]. The metallurgical causes of the high susceptibility of segregation-induced hot cracks are mainly the low solubility and diffusion rate of polluting elements such as sulfur, phosphorus, and boron in the face-centered cubic lattice structure of the Ni-based alloys. The quantity and morphology of the segregations and low melting phases influence the hot cracking. Consequently, a high number of polluting elements increase the risk of hot cracking. However, inclusions in the material can also have a favorable effect on the morphology of the grain boundary films and on the grain size. A finer solidification structure and the transition from film to the globular form of the unwanted contaminants may even increase the hot crack resistance in some cases [4–6].

Other reasons for the high hot crack sensitivity of Ni-based alloys are:

- The high thermal expansion with low thermal conductivity, which results in larger strain and shrinkage reactions in the temperature range of hot cracking [7],
- The mostly cellular solidification of the weld metal, which supports the formation of segregation-induced hot cracks [4], and
- Low ductility at high temperatures, which results in higher thermal stresses [8].

Other typical weld imperfections of Ni-based alloys are lack of fusion or porosities. The lack of fusion occurs because of the very viscous melt and the associated awkward flow and wetting behavior. A sufficiently high temperature at the weld flanks has a favorable effect here [9].

Recommended for publication by Commission II - Arc Welding and Filler Metals

✉ Stefan Burger
stefan.burger@ovgu.de

Manuela Zinke
manuela.zinke@ovgu.de

Sven Jüttner
sven.juettner@ovgu.de

[1] Institute of Materials and Joining Technology, Otto von Guericke University, Universitätsplatz 2, 39106 Magdeburg, Germany

The approaches to avoid hot cracking result from the abovementioned influencing factors. From a metallurgical point of view, the degree of purity of Ni-based alloys is said to have a significant effect on the material and welding properties and thus on the hot cracking tendency [10, 11]. With the use of basic flux-cored wires, hot crack supporting elements such as sulfur, phosphorus, and boron react with slag and can be reduced [12, 13, 17]. Furthermore, basic flux-cored wires should bring significant benefits compared to rutile slag due to deoxidizing effects. Thus, in the literature, a lower oxygen content in the weld metal of basic flux-cored wires is mentioned resulting in less oxidic inclusions and better mechanical properties.

Flux-cored wires were standardized in ISO 12153 [14]. In comparison to solid wires, flux-cored wires have some technological benefits. In the literature [9, 15–19], these include a simple handling for welders, high welding process stability even without pulsed arc technology, a large parameter window, the use of low-cost standard mixed gases (M21) and welding power sources, a very low weld oxidation, and deep penetration. For GMAW with solid wires, special argon and helium multi-component mixed gases are used which contain hydrogen (max. 2%) and a low CO_2 addition of 0.05%. The welding of the basic FCW is carried out as in the case of the solid wires, preferably in the position of 1F/1G, 2F. In contrast, the slowly solidifying rutile slag with the letter R allows welding in the position 1F/1G, 2F, and 2G and in vertical positions 3G/5G. With the fast solidifying rutile slag with the letter P, it is possible to weld in all positions.

This paper shall inform about research results about the hot cracking tendency on gas-shielded arc welding with Ni-based flux-cored wires of the type Ni 6625 with basic and rutile slag. In connection with the tendency to hot cracking, the influence of the slag characteristic on the metallurgical processes such as loss or addition of alloying elements is considered. These results will also be contrasted with the results of pulsed GMAW with similar solid wires.

2 Methodology

2.1 Materials and welding process

Table 1 gives a detailed overview of the used Ni-based filler and base materials and their dimensions. In the context of this investigation, rutile FCW from two different manufacturers are used, which are marked following with P* and P**.

The welding investigations were carried out with two inverter welding power sources with the following conditions:

- FCAW: spray arc, standard shielding gas ISO 14175 - M21 (Ar + 18% CO_2)
- GMAW pulsed arc, multi-component shielding gas ISO 14175 - Z (Ar + 30% He +2% H_2 + 0.05% CO_2)

The used welding parameters are based on the setting recommendations of the respective manufacturer (Table 2).

2.2 Characterization of flux-cored wires

In the first step, a fundamental material science examination of the FCW was carried out by using several test methods. To determine the chemical composition of the strips and to identify the filling components, an X-ray fluorescence analysis and an EDX analysis were used at cross sections. The disadvantage of this method is that individual filling components may have fallen out during the preparation of the specimens. Figure 1 shows the procedure of the EDX analysis.

In order to estimate the welding metallurgical processes during GMAW welding, it is important to investigate the shielding gas and slag reactions. With the aim of characterizing the burning lost and pickup behavior in a comparative manner, pure weld metal specimens were prepared as follows:

- GTAW remelting of the filler metals using button-melt technique and
- GMAW and FCAW of 6-layer deposit welds according to method D to ISO 6847 [20]

The experimental principle of the button-melt technique is described in [21]. For this investigation, electrode pieces are remelted to buttons in a furnace with an inert Ar atmosphere by using an arc. In the case of FCW, the melting process must be repeated several times due to slag formation, whereas one melting process is enough for solid wires. The 6-layer deposit welds were produced using shielding gases (M21 and Z) as mentioned above. The determination of chemical compositions of buttons and pure weld metal samples was performed by spectral analysis. In addition, the contents of oxygen,

Table 1 Overview of used base materials and filler metals (Ø 1.2 mm)

Base materials	Alloy short		FCW		Solid wire
(t = 5 or 12 mm)	Numerical	Chemical	Basic B	Rutile P	
NiCr22Mo9Nb alloy 625 (2.4856)	Ni 6625	NiCr22Mo9Nb	X	X	X

Table 2 Used welding parameters for deposit welds and steep-flanked single-V butt joint

	Type of arc	Torch angle	CTWD mm	Gas flow rate l/min	Wire feed rate m/min	Average voltage V	Weld speed m/min	Average current A	Heat input kJ/mm
FCAW	Spray arc	Pull technique	15	18	10.0	28.0–32.0	0.5–0.6	170–220	< 0.8
GMAW	Pulsed arc	Push technique	15	18	8.0	30.0–33.0	0.5–0.6	150–160	< 0.8

nitrogen, carbon, and sulfur of pure weld metal samples were measured using the gas fusion analysis (GFA). The slag of the buttons was also analyzed with EDX. Therefore, the slag of buttons had to be fixed on the sample holder with a self-adhesive carbon pad (Fig. 1b).

In order to determine the mass-related filling degrees, the filling was mechanically separated from the strip and then weighed. The degree of filling was then calculated as the quotient of the weight of the filling and the total mass of the filler metal. Similarly, the electrode efficiency results from the quotient of the mass of the flux-cored wire and the mass of the weld metal. For this purpose, 20 g of untreated filler metal was remelted using the button-melt technique. After the slag was carefully removed from the button, the difference in mass could be determined.

2.3 Evaluation of the hot cracking sensitivity

The evaluation of the hot cracking tendency of the used welding consumables was carried out by using several methods on the basis of externally stressed and self-stressed welded specimens. The programmed deformation rate test (German: PVR test), whose test principle is described in detail in [22, 23], was used as an externally stressed hot cracking test. During the PVR test, the welding is overlaid by a linearly increasing tensile deformation of a flat tensile sample in the longitudinal weld direction. The location on the PVR sample at which the first hot crack occurs corresponds to the critical deformation speed and is directly related to the critical strain rate postulated by Prokhorov's hot crack theory [24]. Generally, the higher the critical deformation speed is, the greater the hot crack resistance.

In our investigations, the PVR test was done in two modified variants highlighted in Fig. 2. In the first variant, a single GMAW bead was welded into a notch machined in a 5-mm-thick sheet of alloy 625. With this variant, only a comparison of the FCW with each other makes sense because, despite constant welding parameters, different heat input per length unit can occur. The reasons are different specific material resistances of FCW as a result of the differences in the proportions of the metallic strip and in the filling components. With the aim of constant welding parameters and minimized process influence, the PVR test was carried out by GTAW remelting of pure weld metal according to ISO 15792-1 [25] of all welding consumables. The advantage of the second variant is that only the influence of the chemical composition of the weld metal on the hot cracking tendency is investigated. Table 3 lists the welding parameters and the sample dimensions.

In addition to the PVR test, all welds were tested for hot cracks as self-stressed samples shown in Fig. 3. Due to the partially adheres slag, no penetrant testing is useful for the FCW welds. For this reason, the cross sections were examined for hot cracks in a polished condition. With the aim of a better

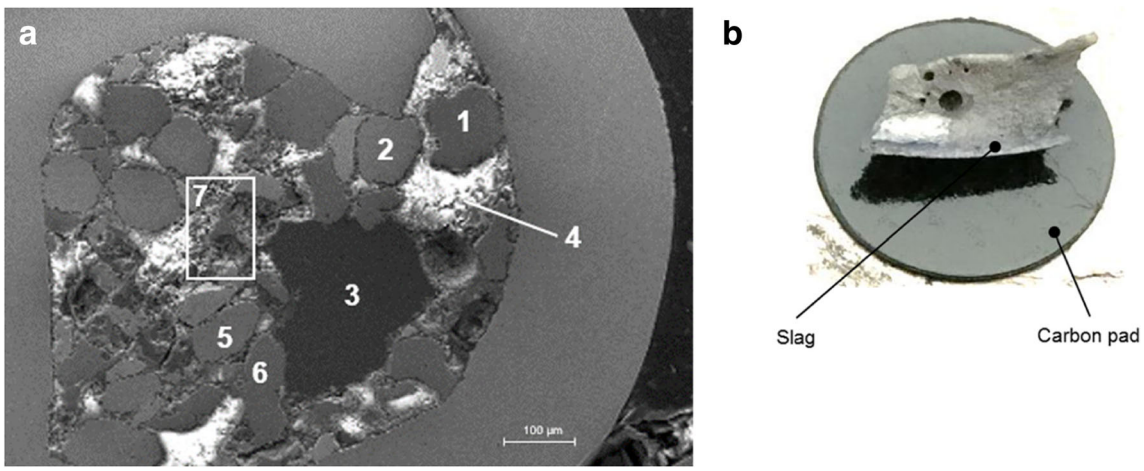

Fig. 1 Procedure of the EDX analyses at the flux-cored wires (**a**) spot analysis of different filling components at the cross section, (**b**) area analysis (100 × 100 [µm]) of prepared slag

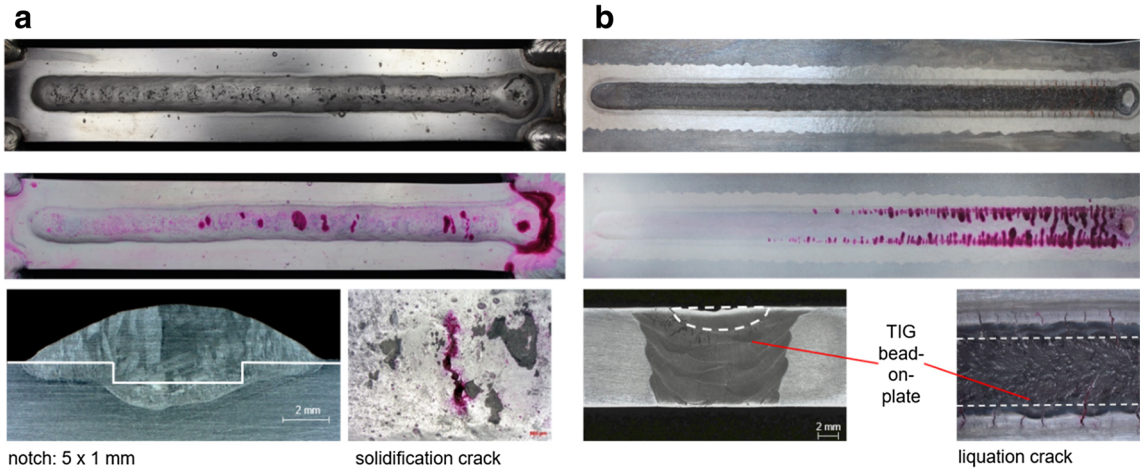

Fig. 2 Variants of the PVR test: single FCAW weld-bead (**a**, variant 1) and GTAW remelting of the pure weld metal (**b**, variant 2)

visualization of the hot cracks, a penetration test was first carried out on the cross sections. The number of cracks (N_{HC}) and lengths was then determined by a stereomicroscope. Then, the crack lengths were summed up and related to a defined measuring area (L_{HC} in µm/mm^2). It should be noted that self-stressed samples should be evaluated as a trend because weld metal blocks cannot be manufactured identically and therefore differences in the level of stress occur.

2.4 Microstructure analysis

The XL30 FEG/ESEM from FEI/Philips was used for the REM-EDX examinations. To investigate the characteristic radiation, the EDAX Si (Li) detector was used. The non-melted FCW were cross-sectioned and hot-mounted in electrically conductive material and then shown in the BSE diagram at up to × 200 magnification. On the basis of the Z contrast, individual measuring points were determined in the filling, and their composition was determined qualitatively using EDX. As can be seen in Fig. 1, the individual measuring points were mainly larger particles (alloying elements). In order to examine the smaller particles, adapted areas (approx. 100 µm^2) were scanned across the surface, and their composition was also examined qualitatively. A quantitative examination of the filling components was useless due to the low informative value.

The REM-EDX investigations on the 6-layer deposit welds and on the steep flank seams were carried out on polished cross sections up to a × 500 magnification. The oxidic inclusions were recorded at five different locations within the weld metal. The oxidic inclusions were often visible even at × 250 magnification. An excitation voltage of 25 kV was used for all EDX examinations. The WDX investigations of the Mo particles were carried out using REM-FIB DualBeam (FEI SCIOS) and AMETEK-EDAX.

3 Results

3.1 Characterization of flux-cored wires

The FCW of Ni 6625 are form-fitted and only differ in the overlap length of the strips depending on the producer (Fig. 4). In consequence, the FCW have different cross-sectional areas of the current-carrying strip, which suggest an influence on the deposition rate due to the different current density. The mass-related degree of filling is between 18 and 24% regardless of the alloy type and slag and resulted in an electrode efficiency (mass ratio of flux-cored wire and weld metal) of 90 ± 3%.

While the strips of T Ni 6625 B (basic) and T Ni 6625 P* (rutile) correspond to the alloy Ni 6625 (N 06625, 2.4856), the strips of T Ni 6625 P** (rutile) correspond to the alloy 80/20 (N 06003, 2.4869) (Table 4). For this reason, the missing alloying elements, such as Nb, Mn, and Mo, are delivered with the filling.

Table 3 Weld parameter of the used variants of PVR test and sample dimensions

Variant	Weld process	Shielding gas (ISO 14175)	Seam type	Sheet thickness mm	CTWD mm	Wire feed rate m/min	Average voltage V	Weld speed m/min	Average current A	Heat input kJ/mm
1	FCAW	M21	Single bead	5	15	10.0	31.0	0.5	167–200	0.62–0.74
2	GTAW	I1	Bead-on-plate	10	-	-	12.0	0.2	180	0.65

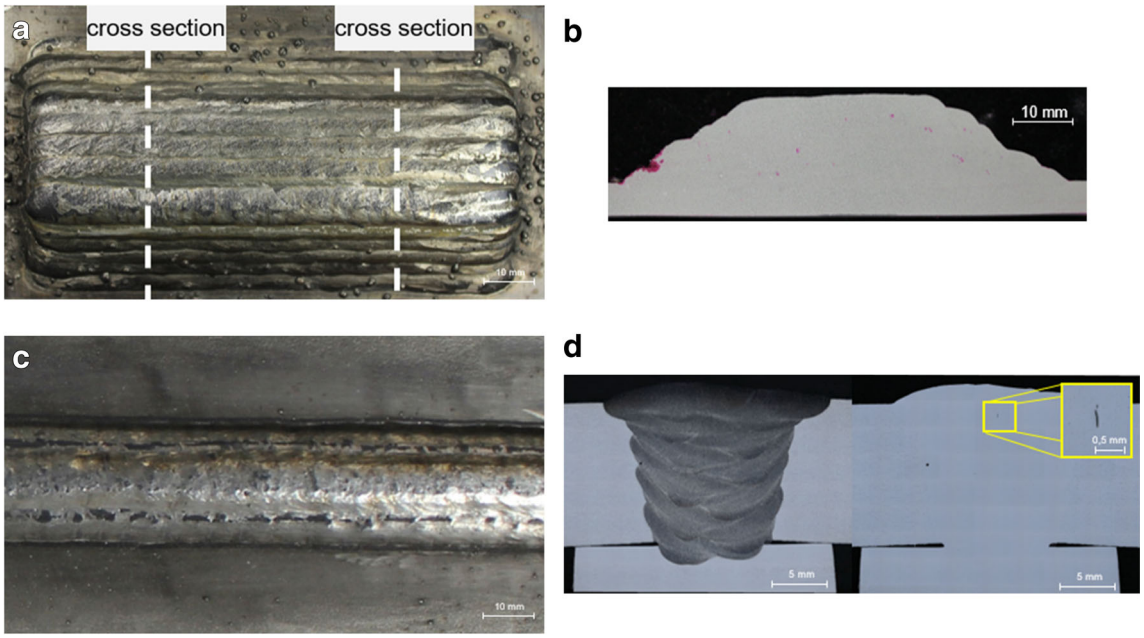

Fig. 3 Evaluation of self-stressed weld specimens. **a** 6-layer deposit GMAW weld (basic FCW). **b** Penetrant testing at cross section. **c** Steep-flanked single-V butt weld, $\alpha = 10°$ (rutile FCW). **d** Cross section with etched (left), polished (right) surface

The slags of all FCW showed different gray values in the backscattered electron image (BSE) on the SEM, which indicates a variety of chemical compositions of the fillings. The displayed quantitative values do not represent absolute values, so they are only shown for qualitative comparison. In addition to the alloying elements, typical basic and rutile slag formers, arc stabilizing, and deoxidizing elements were found. Table 5 gives an overview of the filling elements and their function.

The accurate determination of the degree of basicity of the FCW is not possible without knowing the mass fraction of the filling components. Thus, only manufacturer information on basicity can be considered.

3.2 Chemical compositions of filler metals

The type Ni 6625 filler metals used show only slight differences in the chemical composition (Table 6). For example, FCW T Ni 6625 P** has the lowest Mo, Nb, and Fe content and the highest Ni content and the T Ni 6625 P* has 2% more Cr than other wires. With the exception of the Mo and Nb contents of T Ni 6625 P**, all values are within the specified values of the corresponding ISO standards 12153 [14] and ISO 18274 [27]. Furthermore, the results of the chemical composition show no significant burning loss or pickup of alloying elements in all weldments of the flux-cored wires. A minimal burning loss of Nb can be determined only in some flux-cored wires. This, however, does not lead to a significant undercut of the limit value. In [26], an influence of the Nb content on the hot crack susceptibility of Ni-based alloys (NiCr 70/20, NiCr 70/15) is described. Since there are no significant differences in the Nb contents, no influence on the hot cracking tendency is assumed.

The determined oxygen, nitrogen, and sulfur contents of deposit welds according to Method D to ISO 6847 are shown in Table 7. Due to the reactions occurring during welding between the molten slag and weldment, the weld metal of the FCW contains increased oxygen contents between 665 and 1195 ppm, which can result in an increased appearance of oxidic inclusions. The pure weldments of the basic FCW tend to have slightly lower values than those of the similar rutile FCW. Contrary to the expectations, the Charpy impact tests on the pure weld metal did not show any significant

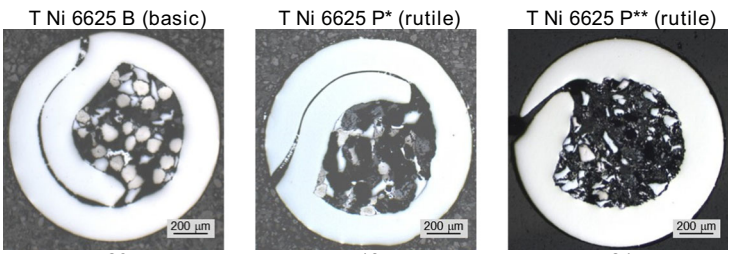

Fig. 4 Cross section of different FCW of type T Ni 6625

Table 4 Chemical composition of fillings and slag of different FCW of T Ni 6625 in wt.-% (X existing)

Materials	Object	Ni	Cr	Mo	Ti	Si	Ca	Na	Mg	F	Al	Zr	K	Mn	Nb	Fe
Alloy 625	Min.	58	20	8	-	-	-	-	-	-	-	-	-	-	3.2	-
	Max.	71	23	10	0.4	0.4	-	-	-	-	0.4	-	-	0.5	3.8	5
T Ni 6625 B basic	Strip	65.50	21.8	8.2	0.2	0.0	-	-	-	-	-	-	-	0.1	3.4	-
	Filling	X	X	X	X	-	X	-	-	X	-	-	-	-	-	-
	Slag	-	4	-	15	9	11	-	4	8	9	-	1	1	4	1
T Ni 6625 P* rutile	Strip	64.7	21.9	8.5	0.3	0.1	-	-	-	-	-	-	-	0.1	3.4	-
	Filling	X	-	X	X	-	-	-	X	-	-	-	-	-	-	-
	Slag	-	20	-	50	-	2	1	3	-	3	20	-	-	-	-
Alloy 80/20	Min.	75	19	-	-	0.5	-	-	-	-	-	-	-	-	-	-
	Max.	-	21	-	-	2.0	-	-	-	-	0.3	-	-	1.0	-	1
T Ni 6625 P** rutile	Strip	79.6	19.9	0	0.1	0.1	-	-	-	-	-	-	-	0.1	0.1	-
	Filling	-	X	X	X	X	-	-	-	-	-	-	-	-	X	-
	Slag	-	23	-	34	4	1	6	1	-	6	14	-	-	11	-

Table 5 Overview of the filling components and their function of Ni-based FCW [29]

Alloying element	Slag formers (according to Boniszewski)		Slag formers (according to melting point)		Arc stabilizing	Deoxydizing
	Basic	Rutile	Fast solidifying	Slow solidifying	Elements	Elements
Mo, Nb, Cr	CaO, MgO, BaO, CaF_2, Na_2O, K_2O, Li_2O, MnO, FeO	SiO_2, TiO_2, Al_2O_3, ZrO_2	CaO, MgO, BaO, Al_2O_3, ZrO_2	CaF_2, Na_2O, K_2O, FeO	ZrO_2, Na_2O, K_2O, Li_2O	CaO, MgO

advantages for the basic flux-cored wires. In contrast, the solid wire weldments have significantly lower oxygen contents at 22 ppm and the highest impact toughness. No sulfur could be detected in the solid wires. Only the basic FCW shows an increased sulfur content of 0.021%, which is above the solubility limit of 0.005% in pure nickel. The remaining nickel is precipitated in NiS. The nitrogen levels show, except for T Ni 6625 P*, no significant differences.

Table 6 Chemical compositions of pure weld metals of different filler metals—determination of carbon with GFA, remaining elements with OES (values in wt.-%)

Filler metal	Object	C	Mn	Si	Cr	Mo	Nb	Fe	Ti	Ni	PREN
ISO 12153 [14]	Min.	-	-	-	20	8	3.15	-	-	58	-
	Max.	0.1	0.5	0.5	23	10	4.15	5	0.4	-	
T Ni 6625 B	GTAW-Button	0.014	0.27	0.27	20.56	8.45	3.98	0.38	0.21	65.70	-
	FCAW weld	0.032	0.27	0.23	20.30	8.55	3.77	0.38	0.21	66.05	49.2
T Ni 6625 P*	GTAW-Button	0.025	0.01	0.36	22.11	8.67	4.30	0.57	0.12	63.68	-
	FCAW weld	0.025	0.01	0.27	22.18	8.63	4.11	0.58	0.26	63.38	51.7
T Ni 6625 P**	GTAW-Button	0.025	0.01	0.50	20.21	7.45	3.57	0.10	0.05	67.99	-
	FCAW weld	0.018	0.01	0.36	20.55	7.34	3.11	0.16	0.09	68.25	45.4
ISO 18274 [27]	Min.	-	-	-	20	8	3.0	-	-	58	-
	Max.	0.1	0.5	0.5	23	10	4.2	5	0.4	-	
S Ni 6625	GTAW-Button	0.006	0.01	0.07	22.20	8.20	4.15	0.14	0.21	64.67	-
	GMAW weld	0.014	0.00	0.07	22.27	8.28	4.19	0.16	0.22	64.48	50.2

Table 7 Results of the gas fusion analysis of samples of deposit welds according to Method D to ISO 6847 [23]

Filler Metal	Contents (average)			Impact toughness at 20 °C (average)
	Oxygen, ppm	Nitrogen, ppm	Sulfur, %	Charpy V-notch J
T Ni 6625 B	665	241	0.021	86
T Ni 6625 P*	1195	341	0.003	83
T Ni 6625 P**	1012	210	0.002	79
S Ni 6625	22	214	0.000	182

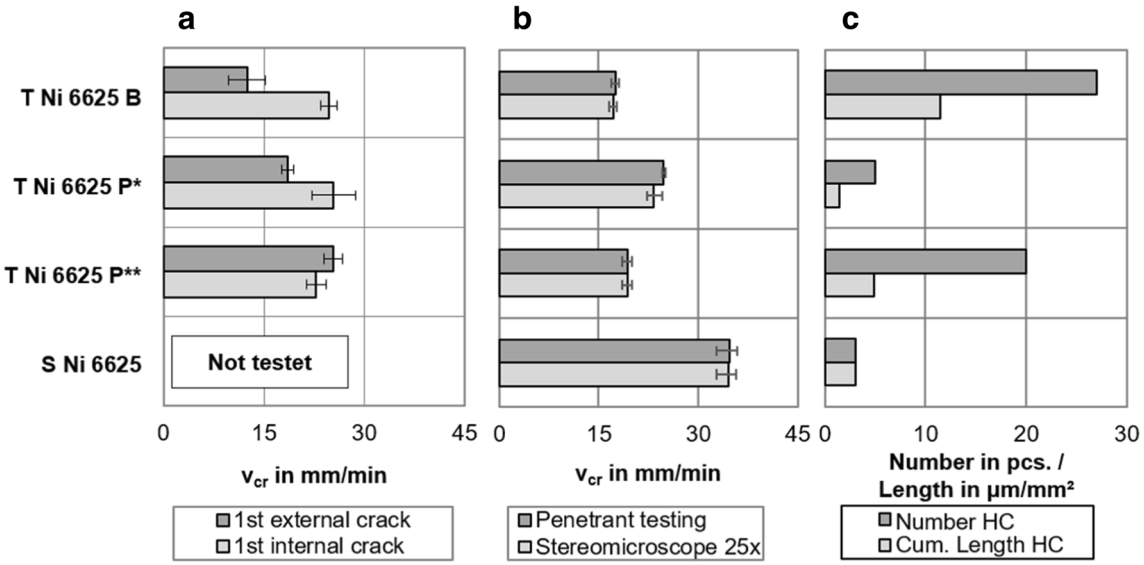

Fig. 5 Results of the programmed deformation rate test of variant 1 (**a**), variant 2 (**b**), and the self-stressed 6-layer deposit welds (**c**)

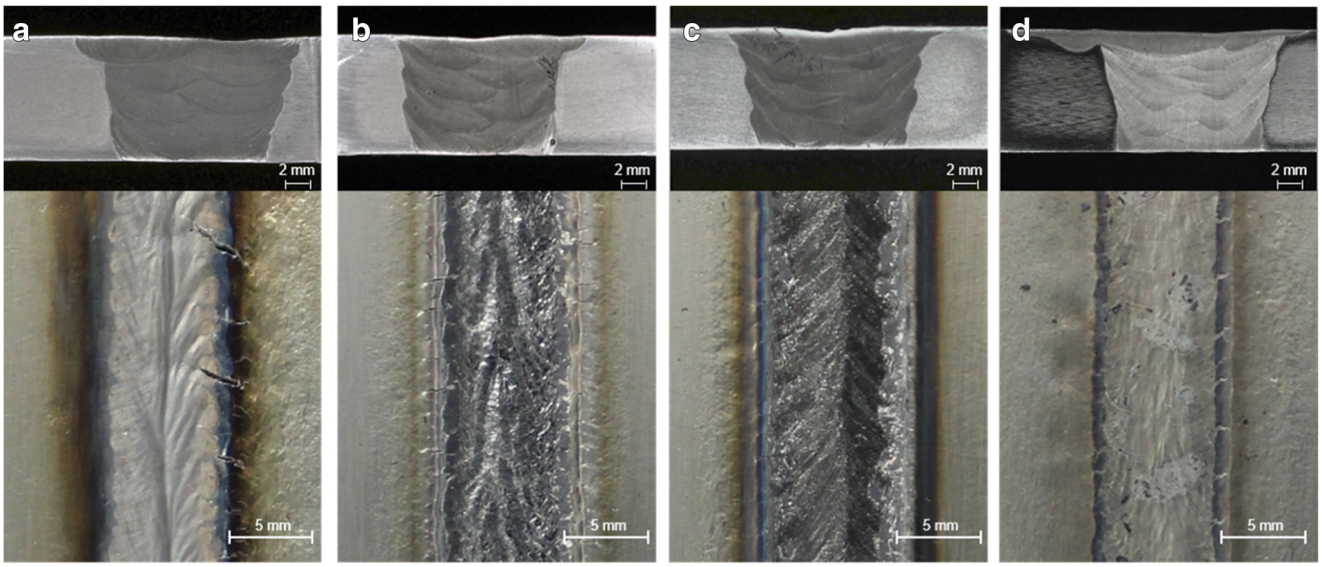

Fig. 6 Cross sections and surface of the PVR sample of different FCW and solid wires—variant 2 (sampling point: 50 mm before the end of the weld). **a** T Ni 6625 B O-content=665 ppm. **b** T Ni 6625 P* O-content=1195 ppm. **c** T Ni 6625 P** O-content=1012 ppm. **d** S Ni 6625 O-content=22 ppm

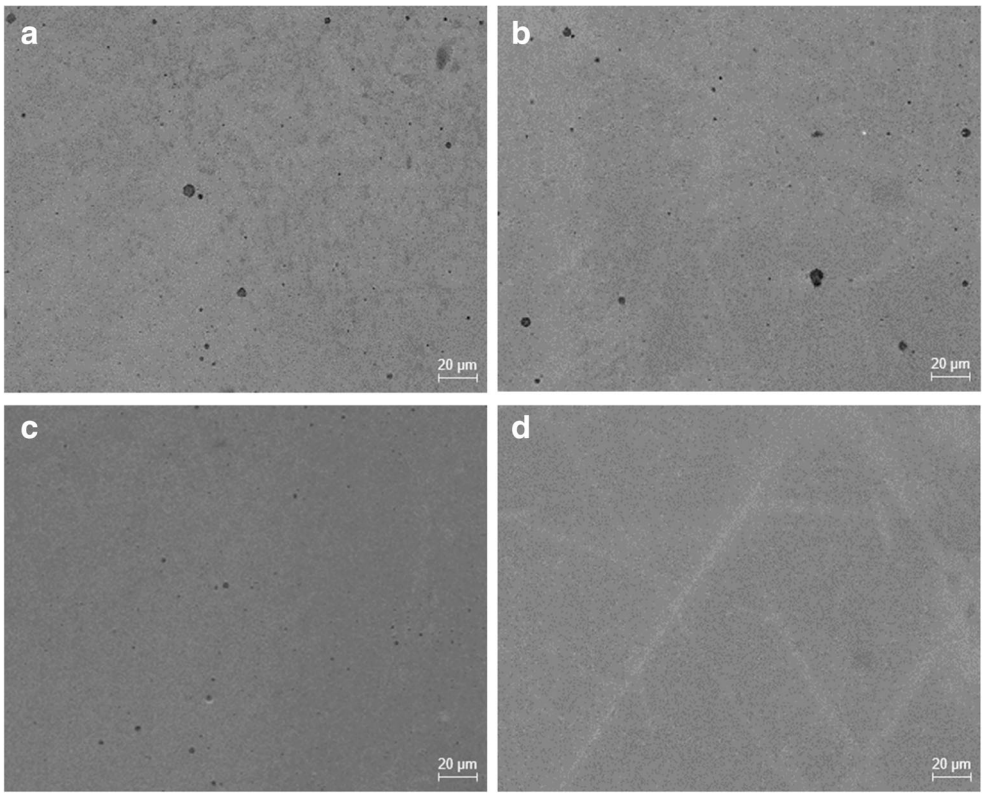

Fig. 7 Comparison of the inclusions with low and oxygen content in the weld metal. **a** T Ni 6625 B, oxygen content = 665 ppm. **b** T Ni 6625 P*, oxygen content = 1195 ppm. **c** T Ni 6625 P**, oxygen content = 1012 ppm. **d** S Ni 6625 (solid wire), oxygen content = 22 ppm

3.3 Hot cracking tendency

For the determination of the externally visible hot cracks in the PVR test in variant 1 (FCAW single weld bead), the strong adhering slag constituents had to be removed without damaging the surface. Subsequent treatment of the samples with liquid nitrogen and simultaneous mechanical brushing made this possible. The detected external cracks were exclusively solidification cracks. Accordingly, the weld beads of the basic FCW have the highest tendency of the occurrence of solidification cracks (Fig. 5a). Subsequently, the weld beads were milled on plate-level to determine the critical deformation rate for the internal hot cracks. Accordingly, the inner cracks occur later than the outer cracks and show no significant influence of the slag on the hot crack tendency.

The PVR tests of the samples of the GTAW remelted pure weldment (variant 2) could be examined for hot cracks directly after cleaning with the help of the penetrant test and stereomicroscope due to the missing slag. The results in Fig. 5b show that the solid wires have the highest hot crack. When comparing the different types of slag, the assumed higher hot crack resistance of the basic FCW could not be confirmed.

In addition to the formation of low-melting phases, a high sulfur, oxygen, or nitrogen content also causes a high-temperature gradient on the surface of the weld pool and thus leads to the Marangoni effect. The resulting deeper and tighter

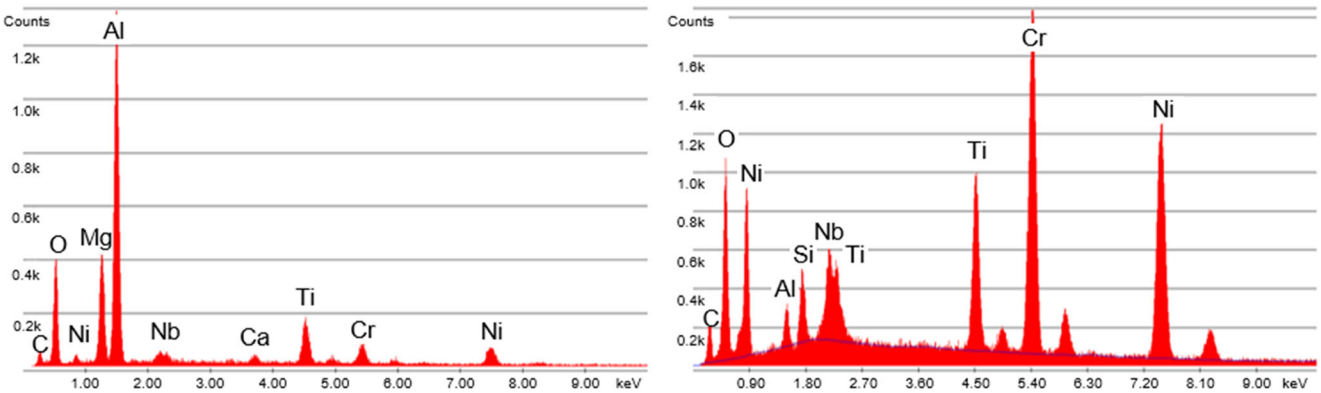

Fig. 8 EDX spectrum of mixed oxide. **a** T Ni 6625 B. **b** T Ni 6625 P**

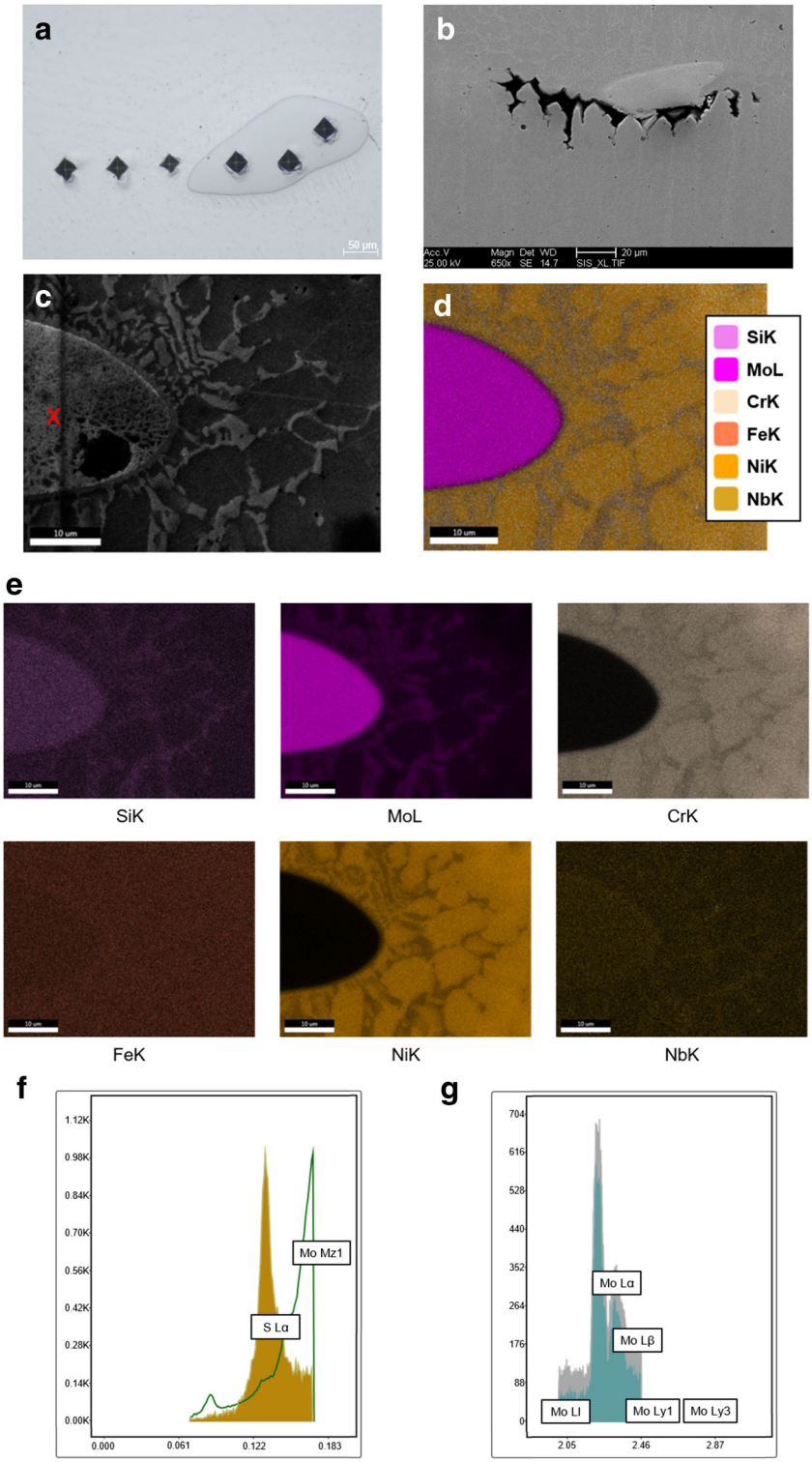

Fig. 9 Examination of the located Mo particles of pure weldment of Ni 6625. **a** Grey Mo particle with hardness measuring points. **b** Mo particle and crack located with REM. **c** Area of EDX-mapping and WDXS-spot. **d** EDX-mapping – element overlay. **e** EDX-mapping – individual view. **g** Comparison of the X-ray spectrum of the Mo phase with a sulfur-containing reference sample

seams tend to accumulate contaminants in the middle of the seam due to the inward solidification and may have a negative influence on the susceptibility to hot cracks [11, 28]. As can be seen in Fig. 6, oxides and a dished seam were found on the surface of the remelted pure weld metal from FCW, which indicates a reduced viscosity of the melt.

Furthermore, Fig. 5c shows the result of the self-stressed investigation. It contains the number [N_{HC}] and the

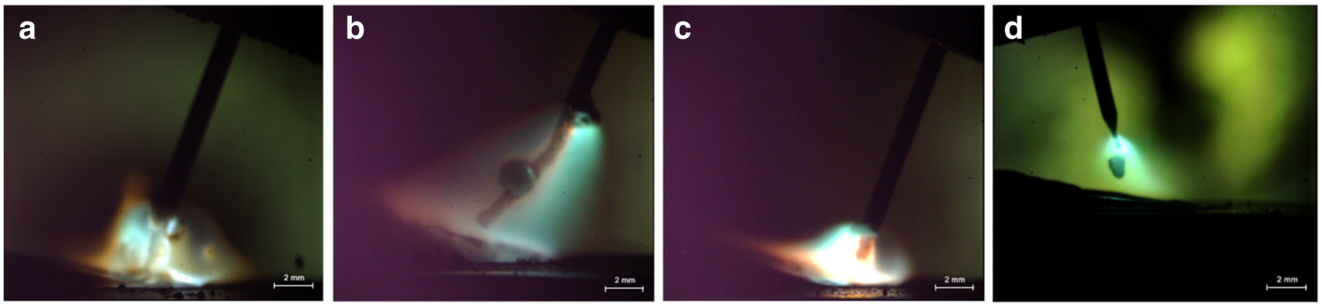

Fig. 10 Comparison of the resulting arcs with the optimized welding parameters from Table 2. **a** T Ni 6625 B. **b** T Ni 6625 P*. **c** T Ni 6625 P**. **d** S Ni 6625

cumulative areal length [L_{HC} in µm/mm^2] of the hot cracks found in the cross sections. Accordingly, the basic flux-cored wires have the highest susceptibility to hot cracking, whereas the rutile flux-cored wires and solid wires have significantly fewer hot cracks in parts. The Ni 6625 solid wire showed hot cracks at a low level.

3.4 Microstructure analysis

Figure 7 shows the correlation between high oxygen contents and oxidic inclusions based on the pure weld metal of the steep flank seams in an exemplary manner. The EDX investigations showed that the inclusions are predominantly mixed oxides and occasionally micro-porosities (Fig. 8). The nitrogen contents result from the alloy type depending on the manufacturer and show no special features. The pure weldments of the basic FCW have the highest sulfur contents independent of the alloy, while the solid wires have very low sulfur and carbon contents.

We also found grey particles in the polished cross sections of the steep-flanked single-V butt welds with an optical microscope and carried out a measurement of hardness as can be seen in Fig. 9a. The determined hardness values were between 117 HV0.1 and 131 HV0.1 and showed no significant differences between the gray particle and the surrounding matrix. In the transition zone of some particles, the hardness increased up to 168 HV0.1. For more detailed information, an EDX and a WDXS analysis were carried out highlighted in Fig. 9. This has shown that the particle consists of pure Mo without the suspected sulfur content. For this reason, it is assumed that the Mo particles which were found and are introduced Mo particles in the FCW filling as alloying elements, which then only dissolve slowly in the melting. Mo has a very high melting point at 2623 °C and may not have completely melted in the arc, since the arc burned upward on the strip of the FCW and the slag may have an isolating effect shown in Fig. 10. This assumption is also supported by the fact that no Mo inclusions could be found in the welds with the solid wire.

Table 8 summarizes the results of the self-stressed and externally stressed hot cracking tests. For this, a ranking of the hot crack susceptibility was formed for each test method. A weighted overall rating was created for comparative evaluation of the welding consumables. Due to the undefined technological influence on the results, the self-stressed hot cracking tests were each weighted with 10%. The self-stressed hot cracking tests were each weighted with 40%.

It can be seen that the examinations correlate well with a few exceptions. Based on the total rating, it can be concluded that the solid wire, S Ni 6625, has the highest resistance and the basic FCW has the lowest resistance to hot cracking. In

Table 8 Comparative demonstration of the self-stressed and externally stressed hot cracking test

Filler Metal	Self-stressed hot cracking test				Externally stressed PVR test				Total rating of hot cracking
	6-layer deposit welds		Steep-flanked single-V butt joint		V1: single bead		V2: GTAW remelting		
	Number of hot cracks	Rating	Number of hot cracks	Rating	v_{cr}	Rating	v_{cr}	Rating	
	pcs.	-	pcs.	-	mm/min	-	mm/min	-	-
T Ni 6625 B	27	4	7	4	13	3	18	4	3.7
T Ni 6625 P*	5	2	3	3	19	2	25	2	2.1
T Ni 6625 P**	20	3	2	2	23	1	19	3	2.3
S Ni 6625	4	1	1	1	-	-	35	1	1.0

Table 9 Correlating of the determined oxygen and sulfur contents and the number of Mo particles, we found 2 cross sections in the pure weld metal

Filler metal	Number of Mo particles	Rating	Oxygen content	Rating	Sulfur content	Rating	Total rating of hot cracking
	pcs.	-	ppm	-	wt-%	-	-
T Ni 6625 B	13 (2)	4	665	2	0.021	4	3.7
T Ni 6625 P*	12 (1)	3	1195	4	0.003	3	2.1
T Ni 6625 P**	1 (0)	2	1012	3	0.002	2	2.3
S Ni 6625	0 (0)	1	22	1	0.000	1	1.0

comparison, the rutile FCW are in the middle regardless of the manufacturer.

Finally, Table 9 shows the correlation of the determined oxygen, the sulfur contents in the pure weld metal, and the number of Mo particles found in the cross sections with the hot cracking tendency. The number in brackets contains the number of Mo particles with founded cracks as can be seen in Fig. 9a/b. The rating also shows that there is apparently a correlation between the Mo particles found and the hot cracking susceptibility. Since cracks were found in only around 10% of the Mo particles, the Mo particles cannot be the only cause for the higher hot cracking susceptibility of these FCW compared to the solid wires.

With the aim of identifying low-melting phases (like NiS), an analysis of the microstructure is currently being carried out.

4 Summary

The characterization of the welding consumables showed that all flux-cored wires are form-fitted and differ only in the overlap length. This resulted in the comparable filling degree of 18–24% and resulted in an electrode efficiency of 90 ± 3%. With regard to the welding metallurgical processes at FCAW, irrespective of the used welding consumable and shielding gas, no significant burning loss and pickup of alloying elements occur.

The results of the PVR test depend on the used variant. Nevertheless, it can be denoted that the pure weldment of the solid wires has the highest hot crack resistance. This also correlates with the results of the self-stressed hot crack test. Contrary to the original assumptions, the basic FCW showed a higher tendency for the occurrence of hot cracks in the PVR experiments of variant 1 (FCAW weld bead). In contrast, the GTAW remelting of the pure weld metal PVR samples of all welding consumables showed no significant differences when looking at the FCW.

The findings of the self-stressed and externally stressed hot crack test almost correlate with the determined sulfur contents. Thus, the lowest hot-crack susceptibility of solid wires was found to have the lowest sulfur and oxygen content in the pure weldment. This is in contrast to the basic flux-cored wire, which has the highest sulfur and oxygen content and the highest susceptibility to hot cracking. Therefore, it can be assumed that the reaction with the basic slag components (like MnO) is insufficient to remove all the hot crack supporting sulfur from the melt. This may be due to the fact that the degree of filling of the flux-cored wires is too low, so that the reactions may not be complete. Furthermore, the slow-motion videos show that the current-carrying strip melts off before filling, so that the passing drop is not coated by the slag. The chemical reactions (metal/slag) then only take place in the relatively cold melt bath. The located Mo particles in the pure weld metal could be identified as a further influencing factor on the hot crack susceptibility because the number also correlates when considering the filler metals.

Acknowledgments Open Access funding enabled and organized by Projekt DEAL. Equal thanks go to all companies, colleagues, and students who contributed with their support, knowledge, and effort to the project.

Funding The authors would like to thank the AiF for funding the IGF-Project IGF-No. 18.099 B / DVS No. 01.086 of the Association, Research Association Welding and allied processes e.V. of the DVS, Aachener Str. 172, 40223 Düsseldorf, which was part of the program to support cooperative industrial research by the Federal Ministry for Economic Affairs and Energy, following a decision of the German Bundestag.

References

1. Caron JL, Sowards JW (2014) Weldability of nickel-base alloys. In: Comprehensive Materials Processing. Elsevier Ltd. 6th edn., pp 151–179.

2. Yushchenko KA, Savchenko S (2001) Welding of high-nickel alloys: high productivity joining processes, Volume II. 7th International Aachen Welding Conference 2001, pp 677–688
3. Gollnow C, Kannengiesser T (2015) Consideration of welding specific component design and resulting loads on solidification crack initiation. In: Hot Cracking Phenomena in Welds IV, EDX.: Lippold J, Böllinghaus T, Cross CE, Springer, Berlin, pp 101-118
4. Lippold JC, Savage WF (1982) Solidification of austenitic stainless steel weldments: Part III -The effect of solidification behavior on hot cracking susceptibility. Welding Journal, Welding Research Supplement, In, pp 388–396
5. Lippold JC, Baeslack WAI, Varol I (1992) Heat-affected zone liquation cracking in austenitic and duplex stainless steels. Welding Journal, Welding Research Supplement 71:1–14
6. Schuster J (1998) Grundlegende Betrachtung zur Entstehung von Heißrissen. In: Schweißen und Schneiden 50(10):646–654
7. Mandziej ST (2005) Testing for susceptibility to hot cracking on GleebleTM physical simulator. In: Hot cracking phenomena in welds IV, EDX.: Böllinghaus T, Herold H, Springer Berlin, pp 347-376
8. Shankar V, Gill T, Mannan S et al (2003) Solidification cracking in austenitic stainless steel welds. Sadhana – Academy Proceedings in Engineering Sciences 28:359–382
9. Bouquin B, et al (2009) Use of modern nickel-base flux-cored wires in apparatus manufacturing, DVS-Berichte Band 258, Düsseldorf, pp 264-268
10. Hope AT, Lippold JC (2015) Use of Computational and Experimental Techniques to Predict Susceptibility to Weld Cracking. In: Hot Cracking Phenomena in Welds IV, EDX.: Lippold J, Böllinghaus T, Cross CE, Springer, Berlin, pp 67-86
11. DuPont JN, Lippold JC, Kiser SD (2009) Welding metallurgy and weldability of nickel-base alloys. Wiley, Hoboken
12. Datta I, Parekh M (1989) Filler metal flux basicity determination using the optical basicity index. Welding Journal, Welding Research Development, In, pp 68–74
13. Penning O, Mühlbauer H, Bonnel JM (2008) Basische Fülldrähte für Edelstahl und Nickel-Basis-Legierungen – Das fehlende Bindeglied. DVS-Berichte Band 250, Düsseldorf, pp 291-298.
14. ISO 12153:2011: Welding consumables - tubular cored electrodes for gas shielded and non-gas shielded metal arc welding of nickel and nickel alloys - Classification
15. Kawamoto H, et al (2011) Flux-cored nickel-based alloy wire U.S. Patent 2011/0171485 (A1)
16. Sommitsch C, Posch G, Weinberger T, Figner G (2010) Neue Fügetechniken mit höherer Prozesssicherheit. BHM Berg- und Hüttenmännische Monatshefte 155:219–226
17. Posch G, Baumgartner S, Fiedler M (2009) GMA-Welding of creep resistant steels with flux-cored wires (FCAW): perspectives and limitations. Proceedings of the IIW International Conference on Advances in Welding and Allied Technologies. Singapore, pp 619-624
18. Newell WF (2011) Flux-cored wires for high integrity applications. Proceedings from the sixth international conference: advances in materials technology for fossil power plants. Ohio, pp 1030-1044
19. Gross V (2010) Ni-Base Filler Thermanit 625 in Offshore Industry. Boehler Schweisstechnik Deutschland GmbH, Präsentation, Hamm
20. ISO 6847:2013: Welding consumables - deposition of a weld metal pad for chemical analysis
21. Gould EK (2010) Development of constitution diagram for dissimilar metal welds in nickel alloys and carbon and low-alloy steels. The Ohio State University, Master Thesis
22. ISO/TR 17641-3:2004: Destructive tests on welds in metallic materials - hot cracking tests for weldments - arc welding processes - Part 3: Externally loaded test
23. Fink C, Keil D, Zinke M (2012) Evaluation of hot cracking susceptibility of nickel-based alloys by the PVR test. Welding in the World. Vol. 58:37–43
24. Prokhorov N (1962) The technological strength of metals while crystallizing during welding. Welding Production 9:1–8
25. ISO 15792-1:2000 + Amd 1:2011: Welding consumables - test methods - Part 1: Test methods for all-weld metal test specimens in steel, nickel and nickel alloys
26. Posch G, Vallant R, Klagges W, Cerjak H (2007) Influence of Niobium on mechanical properties and hot crack susceptibility of nickel-base cored-wire weld metal type 70/20 and 70/15, Graz
27. ISO 18274:2010: Welding consumables - solid wire electrodes, solid strip electrodes, solid wires and solid rods for fusion welding of nickel and nickel alloys - Classification
28. Ushio M (1991) Mathematical modelling of flow in the weld pool. Welding International 5(9):679–683. https://doi.org/10.1080/09507119109454436
29. Schulze G (2010) Die Metallurgie des Schweißens. Springer, Heidelberg, Berlin